17th World Conference on Earthquake Engineering, 17WCEE
Sendai, Japan - September 13th to 18th 2020

SHAKE TABLE TESTS ON A DAMAGED REINFORCED CONCRETE FRAME STRUCTURE STRENGTHENED WITH COMPOSITE FABRIC

O.A. Petcu[1], I.O. Toma[2], P. Mihai[3], I.S. Enţuc[4], G. Oprişan[5], V.M. Venghiac[6], G. Ţăranu[7]

[1] *Master Student, The "Gheorghe Asachi" Technical University of Iasi, petcu.ozana@yahoo.com*
[2] *Senior Lecturer, The "Gheorghe Asachi" Technical University of Iasi, ionut.ovidiu.toma@tuiasi.ro*
[3] *Associate Professor, The "Gheorghe Asachi" Technical University of Iasi, petru.mihai@tuiasi.ro*
[4] *Senior Lecturer, The "Gheorghe Asachi" Technical University of Iasi, ioana.entuc@tuiasi.ro*
[5] *Associate Professor, The "Gheorghe Asachi" Technical University of Iasi, gabriel.oprisan@tuiasi.ro*
[6] *Senior Lecturer, The "Gheorghe Asachi" Technical University of Iasi, mircea.venghiac@tuiasi.ro*
[7] *Senior Lecturer, The "Gheorghe Asachi" Technical University of Iasi, george.taranu@tuiasi.ro*

Abstract

With the exponential expansion of urban areas around the globe and the ever-increasing number of reinforced concrete (RC) structures serving a variety of functional purposes, their behavior in case of major seismic event has become of great interest to researchers and decision makers alike. Even though such structures were initially designed to ensure certain levels of safety in case of earthquakes, the damage accumulated in a RC structure during its lifetime due to seismic events will ultimately require its strengthening or being retrofitted to comply with the new seismic design regulations.

The paper presents the results obtained from shake table tests on a damaged RC frame structure that was strengthened with composite fabric. The 1/3-scale symmetric structure was designed according to the specifications of European norms and following the guidelines in the national annex for Romania. The "short column scenario" was considered to account for RC frame structures that have partial infill walls. The design flexural capacities of the columns and beams were 14.3 and 21.6 kNm, respectively. This gave a column-to-beam strength ratio of 0.66, which ensures the failure to occur in the area of focus, that is the short column. The model was subjected to a series of shake table tests that resulted in the structure being damaged.

The RC frame was repaired and strengthened. The damage was localized at the level of the short columns. The severely cracked column cross-section was restored by means of a flowable high strength mortar designed to match the concrete strength class C25. The short column and the beam-to-column joint were additionally strengthened with uni-directional basalt fabric bonded to the surface of the concrete with the help of epoxy resin.

The shake table tests consisted in a series of unidirectional horizontal motions starting with a Peak Ground Acceleration (PGA) amplitude of 0.14g and incrementally increased depending on the response of the model to match the amplitude of the shake table motions applied to the initial model. The record was an artificial earthquake based on the Eurocode 8 (EC8) using soil type C spectrum. After each shake table test the fundamental period of vibration of the model was determined as a means of accounting for any internal damage of the structure that may reduce its stiffness.

The experimental results show an almost full restoration of the structural stiffness and an overall increase in the drift ratio.

Keywords: damaged RC frame structure; composite materials; shake table tests; structural stiffness

1. Introduction

With the exponential expansion of urban areas around the globe and the ever-increasing number of reinforced concrete (RC) structures serving a variety of functional purposes, their behavior in case of major seismic event has become of great interest to researchers and decision makers alike. Even though such structures were initially designed to ensure certain levels of safety in case of earthquakes, the damage accumulated in a RC structure during its lifetime due to seismic events will ultimately require its strengthening or being retrofitted to comply with the new seismic design regulations [1, 2].

Fiber reinforced polymer (FRP) composites have emerged as an evolutionary step from conventional / traditional materials. Although at the beginning they were used more often in aerospace engineering, advanced composites are quickly becoming the first choice of designers when it comes to load-bearing structural components for infrastructure applications. These new materials are now being used worldwide for building new structures as well as for the rehabilitation of the existing ones [3]. FRP materials, including carbon, basalt, glass and aramid FRPs, possess excellent properties, such as high tensile strength, high stiffness, corrosion resistance and light weightiness [4].

Significant research efforts have been invested in assessing the flexural and shear behavior of reinforced concrete beams strengthened with externally bonded carbon fiber-reinforced polymer composite [5]. During seismic event, columns are considered to be vital for the overall stability of the structures because they are expected to resist the lateral cyclic loads induced by the earthquake while also being able to resist the gravitational loads. Composite materials, once again, proved their effectiveness [6] in strengthening the already damaged columns due to either past seismic events or environmental stressors such as chemical attacks [7]. Recent studies conducted on shake tables have shown the benefit of using such composite materials in either retrofitting damaged RC structures [8] [8] or strengthening sub-standard RC frames [9, 10].

One of the major obstacles to the advancement of knowledge regarding the seismic behavior of existing RC frame structures is the lack of experimental data documenting the realistic dynamic responses of structures tested under real or artificial seismic loads [11]. In recent years, several shaking table tests have been performed to assess the seismic behavior of RC frame structures and some of the tests were conducted even up to the structural collapse [12, 13].

Seismic response of RC framed structures has been one of the major topics of interest among the structural engineering researchers around the world [14]. The main reason behind this interest is the complex behavior of the RC structures and their vulnerability to earthquakes [15]. Reinforced concrete frames with infill walls can be frequently found in earthquake-prone areas around the world. Infill walls are commonly considered as non-structural elements and, therefore, are often ignored in the structural analysis and design in terms of their added stiffness to the entire structure. However, they interact with the bounding RC frame under seismic excitations and can have an important influence the load-resisting mechanism of the structural system [16]. Earlier studies [17] and more recent works [18] showed that infill walls lead to significant increases in strength and, especially, stiffness in comparison to bare RC frames with beneficial effect of reducing the deformations induced by the ground motions.

Experimental studies also showed a reduction in the ductility of the infilled RC frame with respect to the bare frame. Moreover, partial infill walls may inadvertently lead to the occurrence of short columns thus creating a new set of problems that requires the attention of the civil engineer, Fig. 1, [19]. Such elements are incorporated into structures either as part of the original design or as a result of the changes that took place during the life time of a building. Members that were originally conceived as short columns may not pose significant problems when subjected to seismic loads since every precaution has been taken during the design stage. However, there are cases when, due to later changes in the layout of the structure, the original slender columns become short. This may be the case of non-structural enclosure walls, partial infill walls that shorten the effective length of the column leading to important changes in its behavior during a seismic event.

The paper presents the results obtained from shake table tests on a damaged RC frame structure that was strengthened with composite fabric. The 1/3-scale symmetric structure was designed according to the specifications of European norms and following the guidelines in the national annex for Romania. The "short column scenario", as seen in Fig. 2, was considered to account for RC frame structures that have partial infill walls.

Fig. 1 – Collapsed short-column during the 2003 earthquake in Algeria [19]

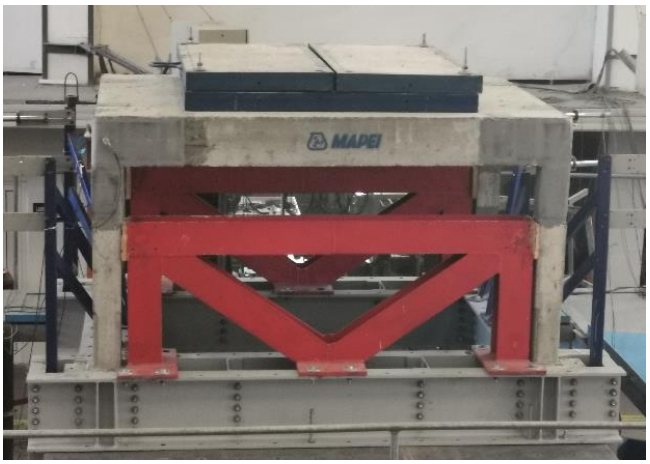

Fig. 2 – Designed experimental model to simulate short-column behavior

2. Materials

2.1 Concrete

A C25/30 concrete strength class was considered as it represents one of the most widely used types of concrete in the construction industry. The mix proportion is shown in Table 1. Natural aggregates with rounded edges were used in order to avoid the occurrence of stress concentrations during the hydration process of cement, thus leading to premature cracks in the concrete. The maximum size of the aggregate was 16 mm. A CEM I – 42.5R rapid hardening cement, readily available on the market, was used in the concrete mix. The average compressive strength, obtained from uniaxial compression tests [20] on 9 cylindrical specimens (100 mm x 200 mm), was $f_{c,14}$ = 32 MPa and $f_{c,28}$ = 35 MPa at 14 days and 28 days, respectively. The corresponding static moduli of elasticity [21], computed as an average of 8 measurements, were $E_{c,14}$ = 32.68 GPa and $E_{c,28}$ = 34.03 GPa [22].

Table 1 – Mix proportion of C25/30 concrete [22]

Cement CEM I 42.5R	**Water**	**W/C**	**Aggregates**		
			Sand	**Sort 4-8 mm**	**Sort 8-16 mm**
[kg/m^3]	**[kg/m^3]**	**-**	**[kg/m^3]**	**[kg/m^3]**	**[kg/m^3]**
489	230	0.47	582	388	647

2.2 Reinforcement

The longitudinal reinforcement was made of BST500 steel, ductility class C, commonly available and used on the construction market. The yield and ultimate tensile strengths were determined by means of direct tensile tests. Their values were f_y = 513 MPa and f_u = 626 MPa for the yield and ultimate strengths, respectively [22]. The shear reinforcement (stirrups) was made of Grade250 steel.

2.3 Composite material and repairing mortar

The damaged short columns were repaired by means of MAPEGROUT HI-FLOW fiber reinforced mortar. The retrofitting process is described in the subsequent section. According to the data sheet supplied by the

producer, the flexural tensile strength at 28 days is 12 MPa and the modulus of elasticity in compression is 27 GPa.

The basalt fiber reinforced polymer (BFRP) strengthening solution consisted in a unidirectional high strength basalt fiber fabric that was applied for the short columns, the ends of both longitudinal and transversal beams and the node of the RC frame structure. The mechanical properties of the basalt fibers and of the composite material are shown in Table 2.

Table 2 – Material properties of the FRP composite (as supplied by the producer)

Basalt fabric – MAPEWRAP B-UNIX-AX-400			**FRP composite – fabric + MapeWrap 21 resin**		
Mass	**Tensile strength**	**Tensile modulus of elasticity**	**Tensile strength**	**Tensile modulus of elasticity**	**Elongation at failure**
[g/m^2]	**[MPa]**	**[GPa]**	**[MPa]**	**[GPa]**	**[%]**
400	2500	70	2300	70	2.5

3. Experimental Program

3.1 Geometry of the model

The geometry of the model in shown in Fig. 3. The building model was a one-bay one-storey frame, with a storey height of 1360 mm and in-plane dimensions of 2550×1950 mm. The slab was 60 mm thick and was reinforced with steel mesh with the diameter of 5 mm spaced at 100 mm in both directions. The columns had a cross-section of 150×150 mm, reinforced with four 14 mm bars as longitudinal reinforcement, and 4 mm stirrups spaced at 100 mm as shear reinforcement [22]. The beams in the X and Y directions, in-plane directions, had a cross-section of 150×260 mm. They were reinforced with four 12 mm and four 10 mm bars respectively as longitudinal reinforcement and 6 mm stirrups spaced at 100 mm in the shear spans and at 200 mm in the middle for both beams.

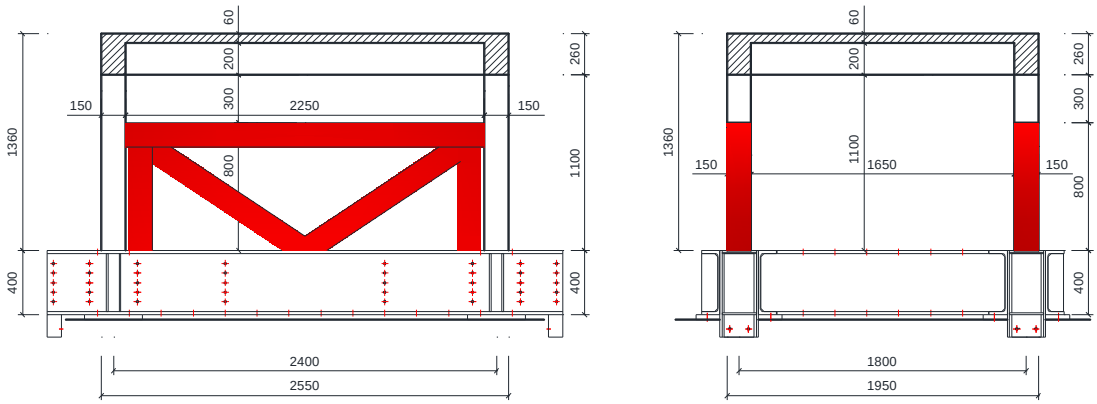

Fig. 3 – Geometry of the model (steel frame to simulate the infill wall is shown in red)

3.2 Strengthening of the model

The initial model was subjected to a series of shake table tests to assess its behavior to seismic motions. The obtained results are presented in [22]. Following these initial tests, the repairing and strengthening of the damaged model and subsequent testing on the shake table came as a solution to simulate one possible real-life scenario.

The cracked concrete was removed from the short columns, exposing the longitudinal reinforcement. The reinforcement was inspected for bents or unusual deformations and the recorded values of strains were checked in order to make sure the reinforcement did not reach its yielding plateau. The reinforcement was

then painted with passivating agent to prevent it from possible rusting before the high-flow fiber reinforced mortar would be cast or by coming in contact with the mortar itself, Fig. 4a.

The corners of the nodes were abraded in order to obtain a rounded shape with the radius of 2.5 cm, similar to the one used in the short columns. The rounding of the corners, for the columns, was obtained by placing in the casting mould four chamfered battens with a radius of 2.5 cm. This was done in order to ensure that the confinement would work as intended and that there were no gaps between the fabric and the column or the node of the model, especially at the corners.

The BFRP was applied at the short columns and on the exterior sides of both the longitudinal and the transversal beams. The BFRP on the beams was used over a length of 300 mm from the face of the columns, Fig. 4b. A supplementary collar was considered over the last 100 mm of BFRP in order to ensure the anchorage. The collar was placed over the three sides of the beam: exterior, bottom and interior side, as seen from Fig. 4c.

a. Reinforcement b. BFRP at the node c. Collar for the anchorage (inside view)

Fig. 4 – Repairing and strengthening of the model

3.3 Instrumentation and loading scenarios

The RC frame had an estimated mass of 1.6 tones. The columns were restrained in the direction of the seismic motion so that to obtain a short column with a height of 300 mm. A prefabricated steel frame, as shown in Fig. 3, was fitted between the columns to simulate an infill wall. Soaked wooden planks were placed at the contact points between the concrete and steel frame to fill the gap so as to avoid local crushing from pounding. Gravity load was provided via 4 concrete slabs, Fig. 2, fixed at the top of the slab, transferring a total of 2.8 tones (self mass and additional load).

The frame was designed to exhibit shear failure in the short columns, to simulate real life cases when columns, initially designed as long slender ones, are restrained along their height due to partial infill walls. The model was equipped with PT5AV displacement transducers to record the lateral displacements of the shake table (1 measuring point) and the top of the structure (4 measuring points), Fig. 5, and Dytran 3202A1 high accuracy accelerometers, Fig. 6. In addition, the lateral displacements of the top and bottom sections of the short columns were recorded by means of LVDTs.

Generally, shake table experiments use one of the following wave forms: sine-beat, sine sweep, time history, continuous sinusoidal input. According to previous observations reported in the scientific literature, if there was no significant coupling between the orthogonal test axes of the specimen, single axes testing with sine beat is the preferred method of testing [23, 24]. The frame was tested using uniaxial shaking with an initial reference Peak Ground Acceleration (PGA) of 0.1g. The initial input signal was a sine-beat function with a duration of 30 seconds. Two distinct input frequencies were used, 1 Hz and 5 Hz, and the

amplitude of the shaking was scaled up with respect to the reference case so that to cover a wide range of significant seismic motions. In order to match the previous testing program [22], the model was subjected to an artificial earthquake with an initial PGA of 0.14g, generated according to Eurocode 8, soil Type C spectrum.

Table 3 presents the sine-beat loading scenarios with the corresponding signal amplification factor, given in dB (decibels), and the amplitude of the shaking motion, expressed in terms of g units. The conversion from dB to g units was performed by means of Eq (1):

$$\frac{x}{x_0} = 10^{\frac{Lx}{20}} \quad (1)$$

where x is the amplification factor of the input signal, x_0 is the amplification factor of the initial / reference input signal (0 dB) and it is equal to 1, Lx is the target amplification level of the input signal (in dB).

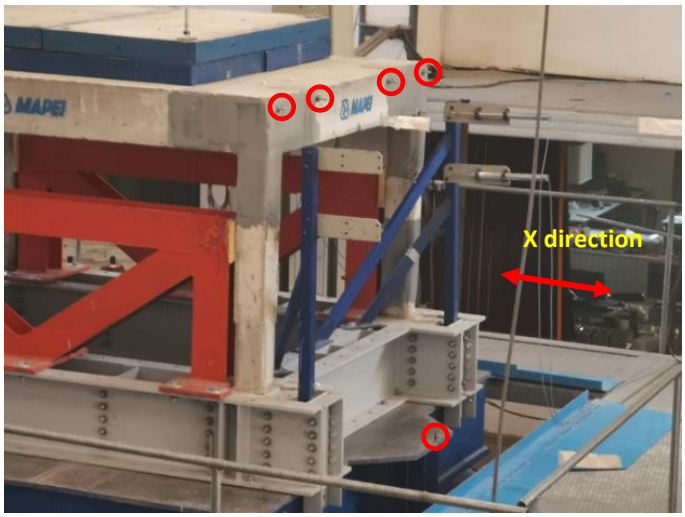

Fig. 5 – Locations of the measuring points for displacements

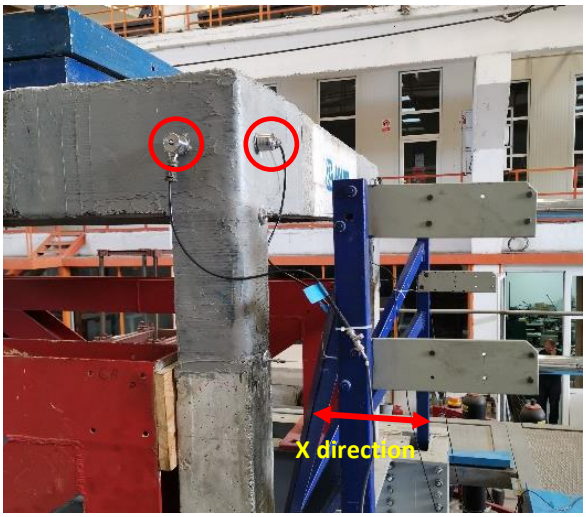

Fig. 6 – Locations of the measuring points for accelerations

Table 3 – Loading scenarios (sine-beat function)

Sine-beat 1 Hz			Sine-beat 5Hz		
Scenario	**Signal amplification [dB]**	**PGA [g]**	**Scenario**	**Signal amplification [dB]**	**PGA [g]**
1Hz_0dB	0	0.10	5Hz_0dB	0	0.10
1Hz_+3dB	+3	0.14	5Hz_+3dB	+3	0.14
1Hz_+6dB	+6	0.20	5Hz_+6dB	+6	0.20
1Hz_+9dB	+9	0.28	5Hz_+9dB	+9	0.28
-	-	-	5Hz_+12dB	+12	0.39
-	-	-	5Hz_+18dB	+18	0.56

4. Results and Discussions

4.1 Lateral displacements

The global lateral displacements were recorded by means of five PT5AV displacement transducers, the locations of which are presented in Fig. 5, for all loading scenarios shown in Table 3 and the artificial earthquake. Fig.7 presents the time history response of the model in terms of lateral displacements for one of the artificial earthquake scenarios. A closer analysis of the obtained results, confirmed later on for all loading

scenarios, reveals the fact that all four displacement transducers recording the displacements at the top of the model, Fig.5, showed similar values for all measuring locations, Fig. 8a. This means that even though the model was subjected to a large number of shake table tests it still follows the uniaxial motion of the seismic input. A comparison of the recorded values for the lateral displacements for the top of the structure and the shake table, Fig. 8b, shows a very small difference between the values which suggests that the structure remains very stiff even at the end of the experimental program.

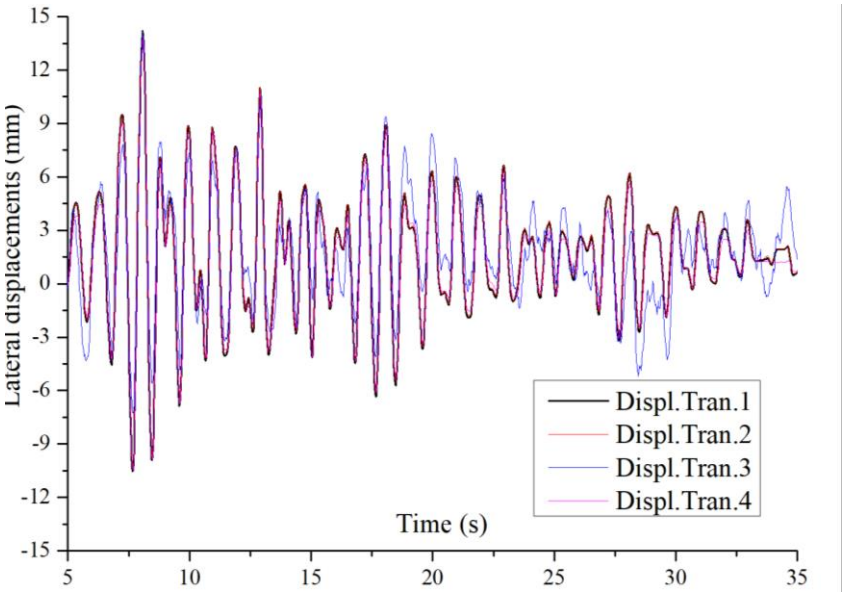

Fig. 7 – Time history response in terms of lateral displacements (artificial earthquake)

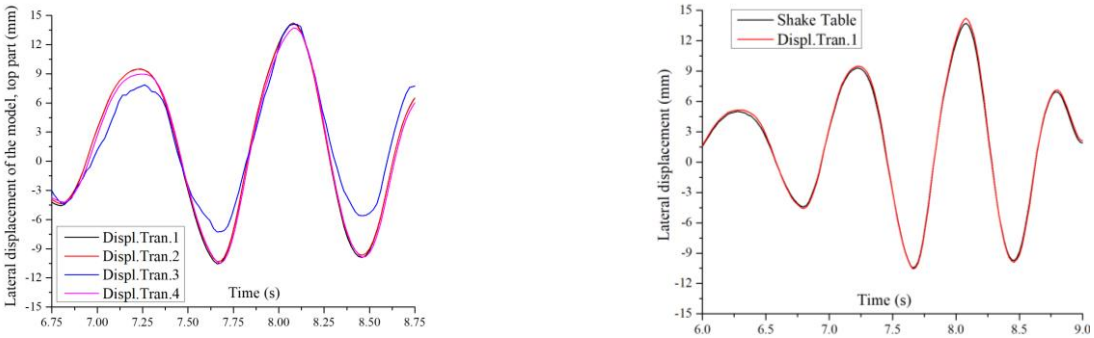

a) measuring points at the top b) shake table and top of the model

Fig. 8 – Comparison of the lateral displacements for the top of the structure and the shake table

4.2 Dynamic properties

A typical response of the structural model, in terms of accelerations, is given in Fig. 9, for the loading case scenario 5Hz_+9dB. The black line is the response of the loop control accelerometer placed under the shaking table and the red line is the recording of the accelerometer placed at the top of the structure in the direction of motion, Fig. 6. After the sine-beat motion is finished the recording of the response was continued for up to 5 more seconds in order to capture the free vibration response. This part of the response signal was used to determine the fundamental frequency of vibration and the critical damping ratio of the structure.

The fundamental frequency of vibration was determined by applying a FFT function for the time domain of the free vibrations response. This method was applied for all loading scenarios presented in Table 3 and the artificial earthquakes.

The damping ratio was assessed by means of the logarithmic decrement. For this purpose, the focus was also on the free vibrations response at the end of each loading scenario. The real response was approximated by a sinusoid function with damping properties, as shown in Fig. 10. The target R-square coefficient for the sinusoidal fitting function was larger than 0.9, meaning a good accuracy of the used function.

The next step consisted in determining the top and lower envelope curves of the fitting function. For this purpose, an exponentially decaying function was considered. The final value of the logarithmic decrement, for a loading scenario, was considered as the average between the values obtained from both lower and upper envelope curves shown in Fig. 10.

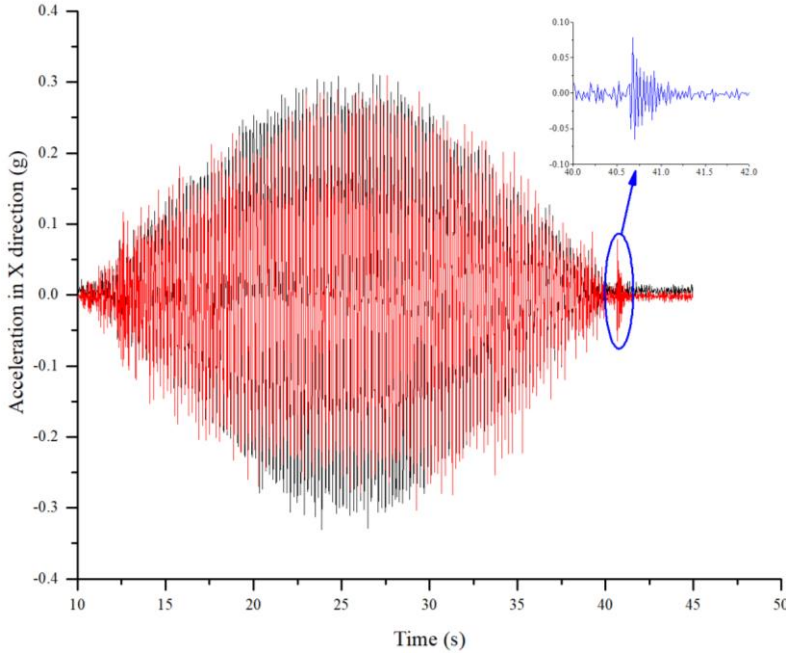

Fig. 9 – Input motion (black) and model response (red) for the 5Hz_+9dB loading scenario

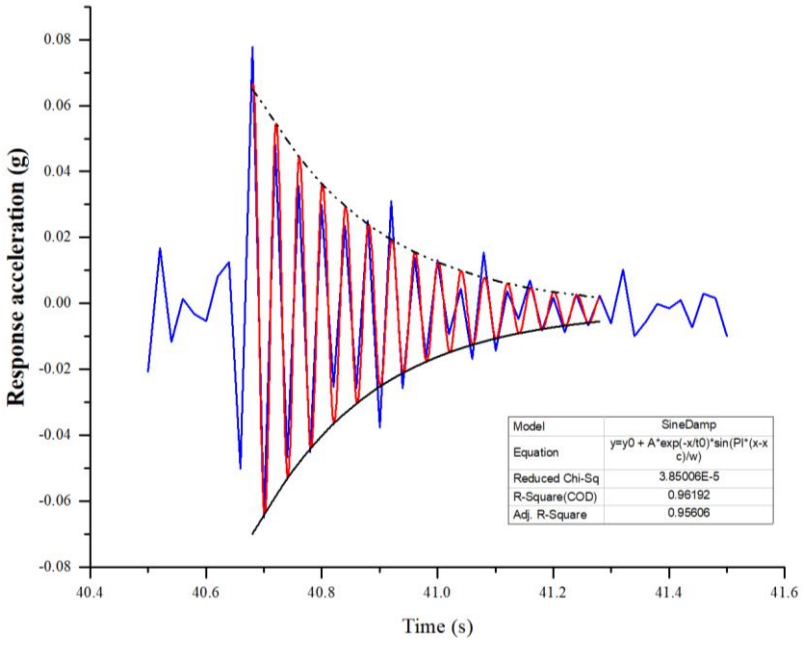

Fig. 10 – Assessment of the logarithmic decrement for the 5Hz_+9dB loading scenario

4.3 Maximum drift in the short columns

The lateral displacements at the lower and top sections of the short columns were recorded during the shaking motions by means of LVDTs, as seen in Fig. 5. The obtained data was used to compute the drift ratio corresponding to the 300 mm height of the short columns. The results are presented in Table 4.

Table 4 – Experimental results (sine-beat function and artificial earthquake)

Scenario	PGA	Fundamental dynamic properties		Damping ratio	Drift ratio
		f	T	ζ	
	[g]	[Hz]	[s]	[%]	[%]
1Hz_0dB	0.10	24.32	0.0411	2.873	0.114
1Hz_+3dB	0.14	24.02	0.0416	2.781	0.128
1Hz_+6dB	0.20	23.91	0.0418	2.688	0.136
1Hz_+9dB	0.28	23.80	0.0420	2.566	0.143
5Hz_0dB	0.10	23.75	0.0421	2.478	0.157
5Hz_+3dB	0.14	23.47	0.0426	2.387	0.159
5Hz_+6dB	0.20	23.17	0.0432	2.266	0.172
5Hz_+9dB	0.28	22.98	0.0435	2.143	0.192
5Hz_+12dB	0.39	22.85	0.0438	2.099	0.210
5Hz_+18dB	0.56	22.71	0.0440	2.041	0.230
EQ_0dB	0.14	22.69	0.0441	1.976	0.232
EQ_+3dB	0.20	22.61	0.0442	1.911	0.240
EQ_+6dB	0.28	22.52	0.0444	1.884	0.250

From Table 4 it can be observed that there is some damage accumulation in the model due to successive shake table motions. A first indication is the increase in the fundamental period of vibration, although by only 8% compared to the initial state of the model, immediately after the rehabilitation process.

A more significant change can be observed in the values of the damping ratio which decreased by as much as 52% from the first shake table test up to the last one. The obtained values for the damping ratio, by means of the logarithmic decrement obtained from the free damped vibrations of the model at the end of each loading scenario, are far from the generally assumed 5% even though the latter is used for creating the response spectrum and it is not generally thought to be the real damping ratio of a RC structure. This is because the damping ratio depends on a large number of factors starting from the quality and soundness of the material a structure is made of and the structural system considered. Some attempts were made to experimentally determine the damping ratio of bridges in Switzerland and Quebec and the obtained values were in the range of 0.5% to 1.45%. Further research should be conducted in this area due to the huge number of parameters and complex mechanical interactions that make the accurate estimation of the damping ratio quite a challenging task.

The short column drift ratio also showed significant changes in its values by as much as 219% from the first to the last shake table test. This may be due to the fact that BFRP was used to confine the repaired short column which greatly increased the stiffness compared to the original model when the short column was unconfined [22]. This lead to the occurrence of cracks in the unconfined part of the column, right below the confinement area, Fig. 11, which may have been the cause of larger difference in reading between the two LVDTs located at the lower and upper sections of the short column.

Upon visual inspection, hairline cracks were identified in all four columns, below the confined area, and at the midspan of all beams, either longitudinal or transversal ones, Fig. 12. This was a visual confirmation of the damage accumulation in the model that confirmed the recorded values for the fundamental frequency of vibration and the calculated values for the damping ratio.

There was no debonding observed between the BFRP and the exterior sides of the beams which proves that the adopted repairing solution was adequate.

Fig. 11 – Damage in the columns

Fig. 12 – Cracking pattern in the longitudinal beam

5. Conclusions

The paper presents the results obtained from shake table tests on a damaged RC frame structure that was strengthened with composite fabric. The 1/3-scale symmetric structure was designed according to the specifications of European norms and following the guidelines in the national annex for Romania. The model was subjected to a series of shake table tests that resulted in the structure being damaged. The damage was localized at the level of the short columns. The RC frame was repaired and strengthened. The cracked concrete from the short column was removed and replaced by a flowable high strength mortar designed to match the concrete strength class C25. The short column and the beam-to-column joint were additionally strengthened with uni-directional basalt fabric bonded to the surface of the concrete with the help of epoxy resin.

The based on the experimental results and the subsequent calculations for the dynamic characteristics of the model, damping ratio and drift ratios in the short columns, the following conclusions can be drawn:

The damage accumulation in the structure is indicated by the decrease in the fundamental frequency of vibration from one shake table test to another. The higher the input motion frequency, the faster the fundamental frequency of vibration decreases.

A similar trend is observed for the damping ratio calculated with the help of the logarithmic decrement obtained from the free damped vibration response of the model at the end of each shake table test. Considering that the mass of the model is constant throughout the entire experimental program, the decrease in the values of the fundamental frequency of vibration is caused by a decrease in the overall stiffness of the structure. This, in turn, leads to less energy being dissipated by internal friction forces and more by means of lateral oscillations. However, due to the huge number of parameters and complex mechanical interactions that make the accurate estimation of the damping ratio quite a challenging task, more research should be conducted in this area.

The short column drift ratio shows significant changes in its values, by as much as 219%, from the first to the last shake table test. The likely cause is believed to be the difference in stiffness between the unconfined part of the column and the short BFRP confined column. Visual inspections reveal the occurrence of a significant number of cracks in the unconfined part of the column, mainly localized immediately below the BFRP confined area.

6. Acknowledgments

The authors acknowledge the partnership with MAPEI Romania, the assistance of Mr. Anton Blidaru in supplying the composite materials and helping with the appropriate placing of the Mapegrout Hi-Flow mortar and Mapewrap B-Unix-AX-400 fabric.

The authors sincerely acknowledge the help of Dr. Mihai-Sergiu Alexa-Stratulat in the operation of the shake-table and data acquisition.

7. References

[1] Xue Q, Wu CW, Chen CC, Chou W (2009): Post-earthquake loss assessment based on structural component damage inspection for residential rc buildings, *Engineering Structures*, **31** (12), 2947–2953.

[2] De Martino G, Di Ludovico M, Prota A, Moroni C, Manfredi G, Dolce M (2017): Estimation of repair costs for rc and masonry residential buildings based on damage data collected by post-earthquake visual inspection, *Bulletin of Earthquake Engineering*, **15** (4), 1681–1706.

[3] Alabdulhady MY, Sneed LH (2019): Torsional strengthening of reinforced concrete beams with externally bonded composites: a state of the art review, *Construction and Building Materials*, **205**, 148–163.

[4] Shang X, Yu J, Li L, Lu Z (2019): Strengthening of rc structures by using engineered cementitious composites: A Review, *Sustainability*, **11** (12), 3384–3402.

[5] Salama ASD, Hawileh RA, Abdalla JA (2019): Performance of externally strengthened RC beams with side-bonded CFRP sheets, *Composite Structures*, **212**, 281–290.

[6] Oprişan G, Enţuc IS, Mihai P, Toma IO, Ţăranu N, Budescu M, Munteanu V (2019): Behaviour of rubberized concrete short columns confined by aramid fibre reinforced polymer jackets subjected to compression, *Advances in Civil Engineering*, **2019**, 1–11.

[7] Rajput AS, Sharma UK, Engineer K (2019): Seismic retrofitting of corroded rc columns using advanced composite materials, *Engineering Structures*, **181**, 35–46.

[8] Ma G, Li H, Wang J (2013): Experimental study of the seismic behavior of an earthquake-damaged reinforced concrete frame structure retrofitted with basalt fiber-reinforced polymer, *Journal of Composites for Construction*, **17** (6), 04013002.

[9] Wang DY, Wang ZY, Yu T, Li H (2017): Shake table tests of large-scale substandard RC frames retrofitted with CFRP wraps before earthquakes, *Journal of Composites for Construction*, **21** (1), 04016062.

[10] Garcia R, Pilakoutas K, Hajirasouliha I, Guadagnini M, Kyriakides N, Ciupala MA (2017): Seismic retrofitting of RC buildings using CFRP and post-tensioned metal straps: shake table tests, *Bulletin of Earthquake Engineering*, **15** (8), 3321–3347.

[11] Li S, Zuo Z, Zhai C, Xu S, Xie L (2016): Shaking table test on the collapse process of a three-story reinforced concrete frame structure, *Engineering Structures*, **118**, 156–166.

[12] Ghannoum WM, Moehle JP (2012): Shake-table tests of a concrete frame sustaining column axial failures, *ACI Structural Journal*, **109** (3), 393–402.

[13] Elwood KJ, Moehle JP (2008): Dynamic collapse analysis for a reinforced concrete frame sustaining shear and axial failures, *Earthquake Engineering & Structural Dynamics*, **37** (7), 991–1012.

[14] Mosleh A, Rodrigues H, Varum H, Costa A, Arêde A (2016): Seismic behavior of RC building structures designed according to current codes, *Structures*, **7**, 1–13.

[15] Sharma A, Reddy GR, Vaze KK (2012): Shake table tests on a non-seismically detailed RC frame structure, *Structural Engineering and Mechanics*, **41** (1), 1–24.

[16] Stavridis A, Koutromanos I, Shing PB (2012): Shake-table tests of a three-story reinforced concrete frame with masonry infill walls, *Earthquake Engineering & Structural Dynamics*, **41** (6), 1089–1108.

[17] Negro P, Verzeletti G (1996): Effect of infills on the global behavior of RC frames: energy considerations from pseudodynamic tests, *Earthquake Engineering & Structural Dynamics*, **25** (8), 753–773.

[18] Benavent-Climent A, Ramírez-Márquez A, Pujol S (2018): Seismic strengthening of low-rise reinforced concrete frame structures with masonry infill walls: shaking-table test, *Engineering Structures*, **165**, 142–151.

[19] Belazougiu M (2003): Boumerdes Algeria earthquake of May 21, 2003: damage analysis and behavior of beam-column reinforced concrete structures, *14th World Conference on Earthquake Engineering (14WCEE)*, Beijing, China.

[20] ASRO (2009): SR EN 12390-3/2009 – Testing Hardened Concrete. Part 3: Compressive Strength of Test Specimens, *Romanian Standards Association*.

[21] ASRO (2013): SR EN 12390-13/2013 – Testing Hardened Concrete. Part 13: Determination of Secant Modulus of Elasticity in Compression, *Romanian Standards Association*.

[22] El Khouri I, Garcia R, Mihai P, Budescu M, Ţăranu N, Toma IO, Gudagnini M, Escolano-Margarit D, Entuc IS, Oprisan G, Hajirasouliha I, Pilakoutas K (2018): Shake table tests on frames made with normal and FRP-confined rubberised concrete, *16th European Conference on Earthquake Engineering (16ECEE)*, Thessaloniki, Greece.

[23] Psycharis IN, Mouzakis HP (2012): Assessment of the seismic design of precast frames with pinned connections from shaking table tests, *Bulletin of Earthquake Engineering*, **10** (6), 1795–1817.

[24] Yavari S, Elwood KJ, Wu CL, Lin SH, Hwang SJ, Moehle JP (2013): Shaking table tests on reinforced concrete frames without seismic detailing, *ACI Structural Journal*, **110** (6), 1001–1011.

